

# The Most Widespread Desmosomal Cadherin, Desmoglein 2, Is a Novel Target of Caspase 3-Mediated Apoptotic Machinery

Nicola Cirillo,<sup>1,2\*</sup> Michele Lanza,<sup>3</sup> Alfredo De Rosa,<sup>2</sup> Marcella Cammarota,<sup>2</sup> Annalisa La Gatta,<sup>3</sup> Fernando Gombos,<sup>1</sup> and Alessandro Lanza<sup>1</sup>

<sup>1</sup>Center on Craniofacial Malformations-MRI, Regione Campania, 1st School of Medicine and Surgery, II University of Naples, 80138 Naples, Italy

<sup>2</sup>Department of Experimental Medicine, 1st School of Medicine and Surgery, II University of Naples, 80138 Naples, Italy

<sup>3</sup>Centro Grandi Apparecchiature, 1st School of Medicine and Surgery, II University of Naples, 80138 Naples, Italy

**Abstract** Apoptotic cells are known to regulate the ordered dismantling of intercellular contacts through caspase activity. Despite the important role of desmoglein (Dsg) 2 in epithelial cell–cell adhesion, the fate of this widespread desmosomal cadherin during apoptosis is yet poorly understood. Here, by means of pharmacological approaches, we investigated whether Dsg2 was targeted by caspases in HaCaT and HT-29 cell lines undergoing staurosporine (STS)-induced apoptosis. Results showed that STS induced a caspase-dependent form of cell-death in both keratinocytes (HaCaT) and enterocytes (HT-29), that associated with progressive depletion of Dsg2 from cell lysates. The proteolytic processing of full-length Dsg2 resulted in the appearance of a 70-kDa fragment which was released into the cytosol. Consistently, immunofluorescence studies revealed that Dsg2 staining was abolished from cell surface whereas the cytoplasmic region of Dsg2 did localize intracellularly. Plakoglobin (Pg) also underwent cleavage and detached from Dsg2. Apoptotic changes paralleled with progressive loss of intercellular adhesion strength. All these biochemical, morphological, and functional changes were regulated by caspase 3. Indeed, in the presence of the caspase 3-inhibitor z-DEVD-fmk, full-length Dsg2 protein levels were preserved, whereas the amount of the 70-kDa fragment was maintained on control levels. Furthermore, cells pretreated with z-DEVD-fmk retained the membrane labeling of Dsg2. Taken together, our data demonstrate that the apoptotic processing of Dsg2 is mediated by caspase 3 in epithelial cells. *J. Cell. Biochem.* 103: 598–606, 2008. © 2007 Wiley-Liss, Inc.

**Key words:** desmoglein; cell–cell adhesion; apoptosis; caspases; staurosporine; keratinocytes; enterocytes; C-HSU buffer

Desmosomes play an important role in cell adhesion and maintenance of tissue architecture within epithelia and a small number of other tissues [Schwarz et al., 1990]. The desmosomal cadherins, transmembrane protein components of desmosomes, mediate adhesion through calcium-dependent homophilic/

heterophilic interactions [Garrod et al., 2002]. The human desmosomal cadherins' family includes four desmogleins (Dsg1-4) and three desmocollins (Dsc1-3), which are expressed in a cell-type and differentiation-specific manner [King et al., 1997; Kljuic et al., 2003]. Dsg2 is the most widespread Dsg, as it is found in all desmosome-assembling tissues including epidermis, gastrointestinal mucosa, heart, and meninges [Schafer et al., 1996]. Some tissues, for example, simple epithelia, express Dsg2 and Dsc2 only. Dsg2 is also the unique Dsg endogenously expressed at high levels by several tumor cell lines [Chitaev and Troyanovsky, 1997].

The crucial role of Dsg2 in development and disease is well established. Mice lacking Dsg2

\*Correspondence to: Dr. Nicola Cirillo, Department of Odontostomatology, Second University of Naples, Via Luigi de Crecchio, 7, 80138 Naples, Italy.  
E-mail: cirillo.sun@libero.it

Received 31 January 2007; Accepted 1 May 2007

DOI 10.1002/jcb.21431

© 2007 Wiley-Liss, Inc.

are unviable, as Dsg2<sup>-/-</sup> mouse embryos die after implantation [Eshkind et al., 2002]. Mutations in DSG2 gene cause arrhythmogenic right-ventricular dysplasia, a heritable form of cardiomyopathy characterized by right-ventricular dysfunction and life-threatening ventricular arrhythmias [Awad et al., 2006]. Abnormal expression of Dsg2 associates to several types of carcinoma, such as gastric and skin cancers [Kurzen et al., 2003; Biedermann et al., 2005].

Programmed cell-death [Lockshin and Williams, 1965] or apoptosis [Kerr et al., 1972], is a genetically regulated process of programmed cell suicide. A dysfunctional apoptotic system can lead to either excessive removal or prolonged survival of cells. Hence, abnormalities in the apoptotic machinery can cause diseases such as cancer [Strasser et al., 1990], promote autoimmunity [Beutler, 2001], and induce tissue-specific disorders [Kaplan, 2004]. Apoptotic cells are characterized by a number of morphological criteria including cell shrinkage, alterations in nuclear morphology, maintenance of membrane integrity, and formation of apoptotic bodies [Saraste and Pulkki, 2000; Hengartner, 2000]. Generally, these events are believed to be mediated by the activation of a family of proteases named caspases [Thornberry and Lazebnik, 1998]. The biochemical features observed during this form of cell-death are dependent on caspase activation and cleavage of specific cellular proteins or "death" substrates within the cell [Hengartner, 2000]. Of these, many are desmosomal proteins, including Dsg1 [Lanza and Cirillo, 2007], Dsg3, Dsc3, desmoplakin (Dpk) I and II, plakophilin (Pkp)-1 [Weiske et al., 2001], and plakoglobin (Pg) [Brancolini et al., 1998]. This probably means that cells undergoing apoptosis must disrupt intercellular contacts by triggering the ordered dismantling of cell adhesion structures. However, recent papers suggest that these events can occur independently of caspase activity, in particular when apoptosis is induced by chemicals such as staurosporine (STS) and cisplatin [Cummings et al., 2004].

So far, the most widespread desmosomal cadherin Dsg2 has not been investigated as a potential target of caspases, although it represents the sole Dsg expressed at high levels in both stratified and simple epithelia. Here, we first assessed whether STS-induced apoptosis works through caspase-dependent mechanisms. Then, we presented an analysis of

the apoptotic changes affecting Dsg2 in both keratinocytes and enterocytes.

## MATERIALS AND METHODS

### Antibodies and Reagents

Rabbit anti-Dsg2 H-145 antibodies against the cytoplasmic domain of Dsg2, the E8A mouse monoclonal antibody against the extracellular domain of Dsg2, K-20 goat IgG to gamma-catenin (Pg), and HRP-conjugated anti-rabbit and anti-mouse antibodies were from Santa Cruz Biotechnology (Santa Cruz, CA). FITC-conjugated anti-rabbit IgG antibodies were from DAKO (Dako Denmark A/S). Nitrocellulose filters were purchased from Invitrogen (Carlsbad, CA); ECL chemiluminescent immunodetection system and Hyperfilms were from Amersham (Buckinghamshire, UK). Caspase inhibitors Z-VAD-fmk and Z-DEVD-fmk were from Calbiochem (Darmstadt, Germany); STS, DAPI, and cell culture reagents and media were from Sigma (St. Louis, MO), except keratinocyte growth medium (KGM), purchased from Gibco BRL (Gaithersburg, MD).

Figures shown in the present paper were representative of at least two independent experiments.

### Cell Cultures and Treatments

For our experiments, we used the HT-29 human adenocarcinoma cell line and HaCaT cells, a nontumorigenic human keratinocyte cell line. Keratinocytes were maintained in serum-free KAD medium [Cirillo et al., 2007] while HT-29 were grown in McCoy's medium plus 10% FBS, both supplemented with penicillin (50 U/ml), streptomycin (50 µg/ml), and fungizone (2.5 µg/ml) in a 5% CO<sub>2</sub> humidified atmosphere. At the time of the experiment, cells were seeded and grown for 3 days in 6-well dishes. Apoptosis was induced by addition of 1 µM STS in DMSO. For inhibitor studies, cells were preincubated for 30 min with 50 µM caspase inhibitors.

### Protein Extraction, Western Blotting, and Immunoprecipitation

Adherent cells were rinsed with complete PBS and scraped in PBS containing the protease inhibitor phenylmethylsulfonylfluoride (PMSF) at 1 mM. Pellets obtained after centrifugation (800g for 10 min) at 4°C were suspended in Cirillo's high salt-urea (C-HSU)

buffer (50 mM HEPES, 800 mM NaCl, 6 M urea, 0.2% Triton X-100, 1 mM DTT, 1 mM PMSF, 10  $\mu$ g/ml leupeptin, and 10  $\mu$ g/ml aprotinin) and stored as whole cell lysates [Cirillo et al., 2007]. In some experiments, cells were subjected to sequential protein extraction, as detailed elsewhere [Lanza et al., 2006].

Protein concentration of samples was determined using Bradford colorimetric assay (Bio-Rad, Richmond, CA). For each lane, 50  $\mu$ g protein mixed with 4 $\times$  SDS sample buffer were separated by 8% SDS-polyacrylamide gel electrophoresis (PAGE), transferred overnight onto nitrocellulose membranes and Western blotting was carried out according to standard procedures [Lanza et al., 2006]. Densitometry values, shown as a mean of independent experiments, were obtained by comparing band intensity with control Dsg2 protein levels (1) after normalization with  $\beta$ -actin as a control.

To immunoprecipitate cytosolic and membrane extracts we followed the procedures reported by us previously [Lanza et al., 2006].

#### Immunofluorescence Microscopy

For immunofluorescence studies, we followed methods published by us previously [Cirillo et al., 2006]. Cells were grown on glass coverslips and treated with 1  $\mu$ M STS for 6 h. After washing with PBS, cells were fixed and permeabilized in 4% paraformaldehyde plus 0.1% Triton X-100 for 10 min on ice and then washed three times in PBS containing 2% BSA to block nonspecific sites. Samples were then incubated with the appropriate primary antibody (1:10) for 1 h on ice, washed in BSA/PBS, and finally exposed to specie-specific antibodies (1:100) conjugated to FITC.

Specimens were examined with a Zeiss Axiophot microscope (Carl Zeiss, Inc., Thornwood, NY) at X 400 magnification and fluorescence images were acquired with an Evolution VF fast digital camera (MediaCybernetics, Marlow, UK).

#### Quantitation of Apoptosis

Apoptosis was assessed by nuclear morphology analysis according to the procedures reported previously [Dusek et al., 2006], with some modifications. Briefly, HaCaT or HT-29 floating or adherent cells were collected 24 h after treatment with STS and fixed in 4% formaldehyde solution for 10 min. Cells were then washed in

PBS and stained with the nuclear dye DAPI (2  $\mu$ g/ml) for 20 min. Condensed/fragmented appearance of nuclear morphology (at least 100 nuclei for sample) was examined by immunofluorescence microscopy with an excitation wavelength of 355–425 nm. Apoptotic nuclei were scored based on the appearance of at least one of three different morphologies: chromatin condensation = chromatin margination without nuclear condensation; nuclear fragmentation = chromatin margination with nuclear condensation; nuclear condensation = nuclear condensation without chromatin margination. The percent cell-death in each sample was calculated based on the following formula: number of apoptotic nuclei / (number of normal nuclei + number of apoptotic nuclei)  $\times$  100. Each experiment was performed in triplicate.

#### Quantitation of Cell-Cell Adhesion

**Morphometric analysis of cell-cell detachment.** The extent of cell detachment in cell monolayers was measured by modifying previously published protocols [Arredondo et al., 2005]. Cells were subjected to immunofluorescence procedures and the images of 10 representative microscopic fields were recorded. The percentage of acantholysis in each field observed by immunofluorescence was computed (Adobe Photoshop) by subtracting the percentage of the area covered by the cells from the total areas of the microscopic field, taken as 100%.

**Cell dissociation assay.** Dispase-based dissociation assay was carried out following standard procedures [Cirillo et al., 2007]. Briefly, cells were exposed to STS for 12 h with or without caspase inhibitors, then media were removed and cells washed three times in PBS. To release monolayers from substrate, both HT-29 and HaCaT were incubated for 1 h in 0.25% dispase. Epithelial sheets were transferred to 15 ml conical tubes containing 4 ml PBS and subjected to mechanical stress by turning tubes upside down 20 times. Cells were returned to Petri dishes and the degree of fragmentation was estimated by counting particles of more than 3 mm.

## RESULTS

### Staurosporine Induces Apoptosis Through Caspase-Dependent Mechanisms

Although STS is a well-known apoptosis inducer, we tested optimal conditions in pilot

assays and then incubated cells with 1  $\mu$ M STS. Changes in morphology, detachment from the substrate, and nuclear condensation (Fig. 1a) demonstrated that keratinocytes responded to the apoptotic stimulus. These findings were also observed and quantified in the HT-29 cell line (Fig. 1b), confirming that induction of apoptosis by STS is not dependent on a specific epithelial cell line. To investigate whether STS-induced cell-death works through activation of caspases in both HaCaT and HT-29, cells were preincubated with the broad caspase inhibitor Z-VAD-fmk. Nuclear condensation was observed in about 70% keratinocytes and 50% enterocytes 12 h after treatment with STS. Conversely, pretreatment with Z-VAD-fmk dropped the amount of apoptotic cells to rates comparable with controls (Fig. 1).

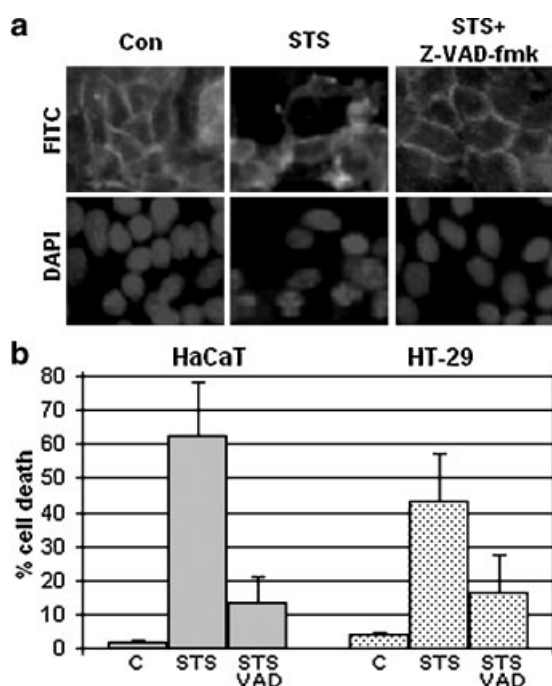


**Fig. 1.** Induction of apoptosis by staurosporine (STS) (a) Within 12 h after treatment with STS, keratinocytes displayed dramatic alterations in both cell and nuclear morphology. As assessed by Dsg3 staining, STS-treated keratinocytes underwent cell shrinkage, changes in cell shape, and ultimately detached from the substrate. These alterations associated with nuclear condensation and fragmentation. These changes were markedly reduced in the presence of the general caspase inhibitor z-VAD-fmk. **b:** For quantitation of apoptosis, nuclei of both floating and adherent cells previously treated with 1  $\mu$ M STS were scored for their condensed/fragmented appearance. Both keratinocytes (HaCaT) and enterocytes (HT-29) responded to the apoptotic stimulus, whereas the induction of cell-death was abrogated by pre-treatment with z-VAD-fmk. Values shown represent the average  $\pm$  SD of two independent experiments.

Taken together, these results demonstrate that STS induces apoptotic changes in epithelial cells via caspase-dependent pathways.

### Dsg2 Processing and Its Progressive Depletion During Apoptosis

The apoptotic fate of Dsg2 was investigated in whole cell lysates by Western blotting. Dsg2 protein was first detected through the E8A monoclonal antibody, which recognizes the extracellular domain of Dsg2. As shown in Figure 2a, the amount of full-length Dsg2 dramatically decreased in a time-dependent manner upon induction of apoptosis. Indeed, Dsg2 was almost completely cleaved within 24 h after treatment with STS, although no low molecular mass proteolytic fragments were revealed (Fig. 2a,c). When instead cell lysates were analyzed with the H145 IgG against the cytoplasmic domain of Dsg2, depletion of full-length Dsg2 paralleled with the appearance of a 70-kDa fragmentation product (Fig. 2b). Quantification of signal intensities showed that the 70-kDa fragment, which was also detectable in normal conditions at lower levels, reached the peak within 1 h after exposure to STS (Fig. 2d). Subsequently, it gradually returned to normal levels within 12 h. The fragment was no more well detectable in cell lysates 24 after STS treatment, probably due to further proteolytic degradation. No changes in the amount of full-length Dsg2 were observed in untreated control cells over the 24-h time course, through neither E8A nor H145 antibodies (not shown). Pg, a cell-adhesion protein which interacts intracellularly with Dsg, was also fragmented in  $\sim$ 55-kDa and  $\sim$ 65-kDa products (Fig. 3a,c), and detached from membrane (Triton X-100 soluble) Dsg2 (Fig. 3b). However, no marked changes in the total amount of full-length Pg was revealed in cell lysates from HT-29 (Fig. 3a). Apoptotic behavior of Pg in HaCaT keratinocytes was comparable to that observed in HT-29 enterocytes (not shown).

### Apoptotic Cleavage of Dsg2 is Mediated by Caspase 3

Members of the Dsg family have previously shown to be targeted by caspase 3 [Dusek et al., 2006; Lanza and Cirillo, 2007]. To test whether formation of the 70-kDa cleavage product of Dsg2 was mediated by this type of protease, we carried out inhibitor studies. In the presence of the caspase-3 inhibitor Z-DEVD-fmk, levels of

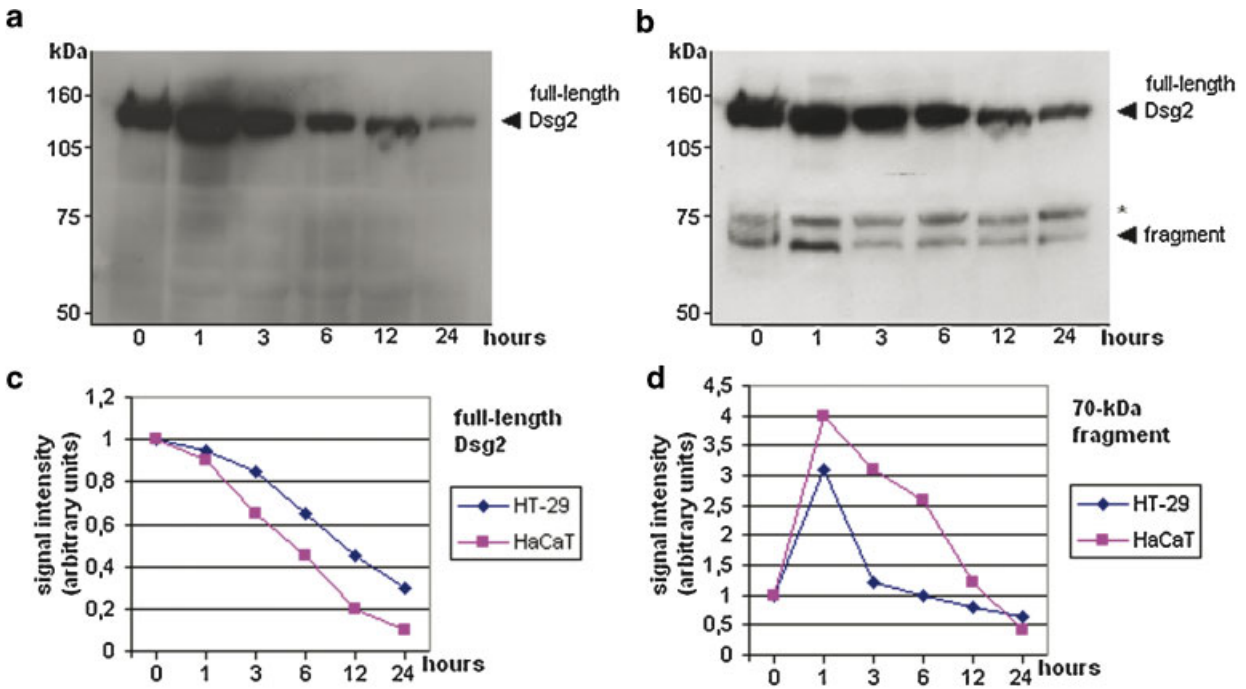


**Fig. 2.** Processing of Dsg2 in apoptotic cells. **a–c:** The amount of Dsg2 protein levels drastically diminished while cells underwent apoptosis, as assessed by E8A (**a**) and H-145 (**b**) antibodies against the external and internal region of Dsg2, respectively. Depletion of full-length Dsg2 from cell lysates paralleled with the appearance of a 70-kDa fragment (**b,d**). The band marked with an asterisk represents an unidentified and unspecific band (**b**). Densitometry values were obtained by comparing band intensities with Dsg2 protein levels at Time 0 (=1) after normalization with  $\beta$ -actin as a control. [Color figure can be viewed in the online issue, which is available at [www.interscience.wiley.com](http://www.interscience.wiley.com).]

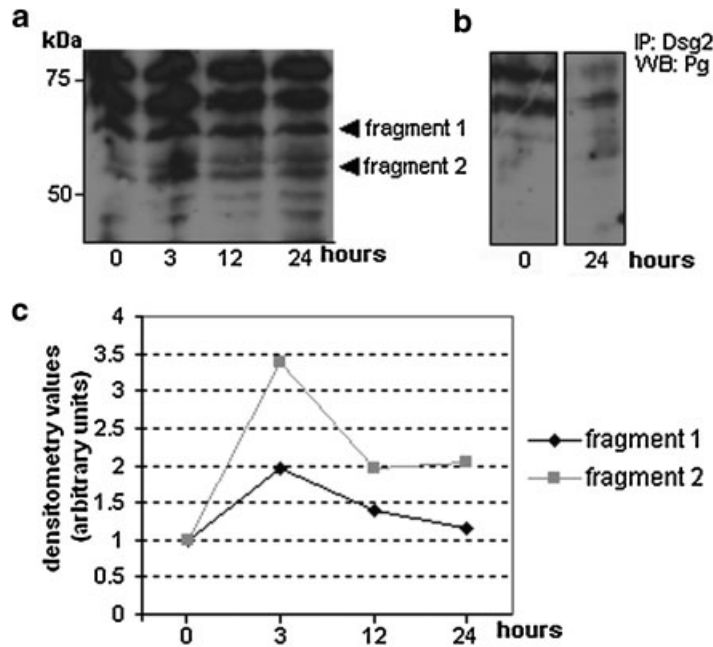


**Fig. 3.** Cytosolic extracts from HT-29 cells were subjected to Western blotting (WB) against plakoglobin (Pg) (**a**). Dsg2 was immunoprecipitated with H-145 IgG from Triton X-100 soluble cell lysates and probed against Pg in WB (**b**). Densitometry values (**c**) were obtained by comparing band intensities with Pg fragment levels at time 0 (1) after normalization with  $\beta$ -actin as a control. Figure represents the typical aspect of bands seen in duplicate experiments.

full-length Dsg2 protein maintained comparable to controls, and formation of the 70-kDa fragment was significantly reduced (Fig. 4a), suggesting that caspase 3 plays a central role within the pathway leading to proteolysis of Dsg2.

The progressive depletion of Dsg2 mediated by caspase 3 was further investigated by immunofluorescence. As the predicted molecular mass of the intracellular domain of Dsg2 is about 75–80 kDa, cleavage of the Dsg2 cytoplasmic domain was expected to release the 70-kDa product within the cytosol. Thus, permeabilized cells were stained with the H-145 antibody recognizing the cytoplasmic domain of Dsg2. Cell-surface Dsg2 was reduced after the onset of apoptosis (Fig. 5), although these changes were more markedly observed in keratinocytes than in enterocytes. Consistently, the reduction of membrane-associated FITC fluorescence was concomitant with the staining of Dsg2 into the cytosol (Fig. 5b,e). These changes were prevented in cells pretreated with Z-DEVD-fmk. Indeed, in the presence of this caspase 3 inhibitor, membrane staining of Dsg2 was preserved, and cytoplasmic localization of FITC fluorescence appeared comparable with controls as well (Fig. 5 c,f).

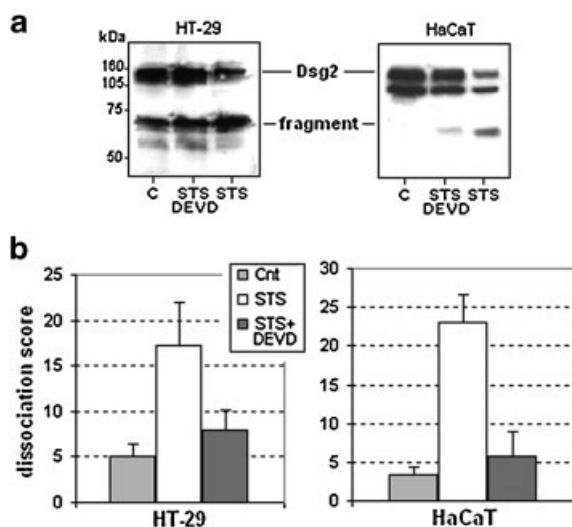


**Fig. 4.** Role of caspase 3 in apoptotic cleavage of Dsg2. **a:** Generation of the 70-kDa fragment was blocked in both HaCaT and HT-29 cell lines in the presence of caspase 3-inhibitor z-DEVD-fmk. **b:** Loss of intercellular adhesion strength in 12 h-STS-treated cells was abrogated by preincubation with z-DEVD-fmk, as revealed by dispase-based assay.

Overall, data from inhibitor studies demonstrate that caspase 3 is the major responsible for cleavage of Dsg2 in epithelial cells undergoing STS-induced apoptosis.

#### Pharmacological Inhibition of Caspase 3-Mediated Pathways Prevents Apoptotic Loss of Cell–Cell Adhesion

Dsg2 plays a major role in establishing intercellular contacts in both enterocytes and keratinocytes. Under morphological means, induction of apoptosis by STS and accompanying cleavage of Dsg2 paralleled with detachment of cells from one another (Fig. 5m). In the presence of Z-DEVD-fmk, however, the rate of cell–cell dissociation dramatically decreased (Fig. 5m).

To test whether apoptotic cleavage of cell adhesion proteins, such as Dsg2, resulted in reduction of the adhesion strength among epithelial cells, we carried out a dispase-based assay. By disrupting cell–matrix interactions without affecting intercellular contacts, dispase enabled us to study the specific changes occurring in cell–cell adhesion. Along the 12-h incubation with STS, keratinocytes underwent dramatic reduction in the strength of intercellular adhesion (Fig. 4b). Apoptosis also affected enterocyte ability in maintaining cell cohesion, although to a less extent if compared with keratinocytes. In both cell lines inhibition of caspase-3 activation by Z-DEVD-fmk drastically reduced the effects of STS in dismantling the integrity of the adhesion complexes (Fig. 5c,f), as the cohesion strength among cells was comparable to controls (Fig. 4b).

Collectively, these data demonstrate that the disruption of cell–cell adhesion in apoptotic epithelial cells is orchestrated by caspase 3.

## DISCUSSION

The apoptotic processing of tissue-restricted Dsg, such as Dsg1 and Dsg3, has been extensively studied in human keratinocytes. Here, we investigated for the first time the fate of the most widespread Dsg, Dsg2, in cells undergoing STS-induced apoptosis. Indeed, although Dsg2 is expressed along with Dsg1, Dsg3, and Dsg4 in keratinocytes, it is the sole Dsg found in simple epithelia, where it plays a critical role in cell adhesion. Results showed that Dsg2 is subjected to apoptotic cleavage mediated by caspase 3. This proteolytic

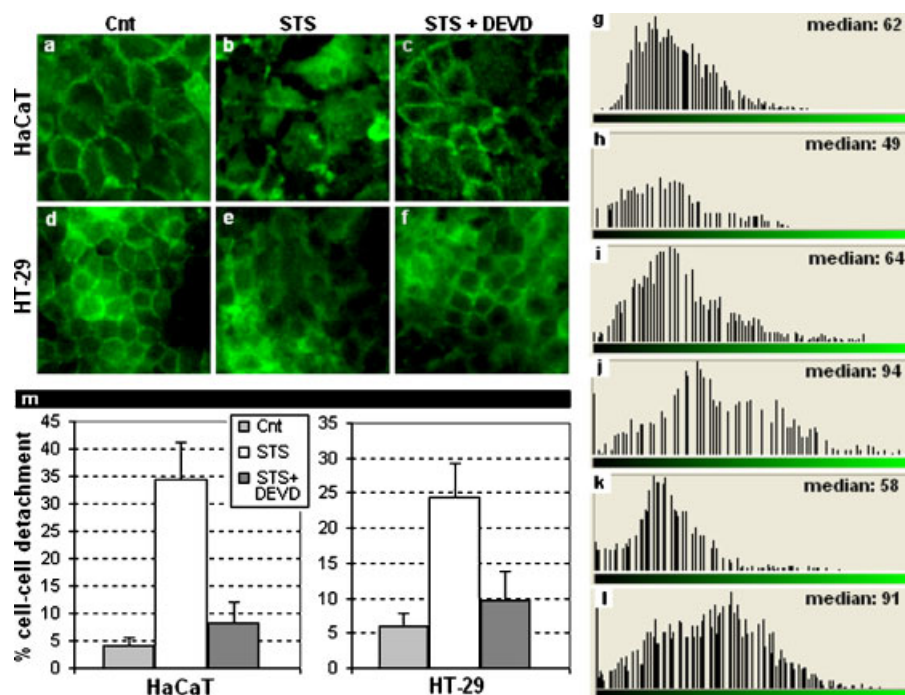


**Fig. 5.** Cell–cell detachment, depletion of membrane-associated Dsg2 and release of its apoptotic fragment within the cytosol. **a,d:** In normal conditions, Dsg2 was labelled mainly on cell periphery. **b,e:** Within 6 h after induction of apoptosis by STS, membrane staining of Dsg2 underwent dramatic reduction. Under these conditions the cytoplasmic region of Dsg2 localized prevalently into the cytoplasm, as assessed by the H-145 antibody. **c,f:** In the presence of z-DEVD-fmk, Dsg2 staining

was overall retained on cell surface. **g–l:** Note that samples were processed simultaneously and photographic procedures held constant to obtain semiquantitative results. Graphs **g–l** refer to as quantitation of fluorescence of the panels **a–f**, respectively (Adobe Photoshop). **m:** Quantitation of cell–cell detachment (see text for details). [Color figure can be viewed in the online issue, which is available at [www.interscience.wiley.com](http://www.interscience.wiley.com).]

processing leads to the formation of a fragment with apparent molecular mass of 70 kDa, which is released into the cytosol.

A number of physiological and pathological stimuli including lack of nutrients, activation of cell-surface death receptors, chemicals, ionizing radiation, and direct physical injury can activate the apoptotic programme [Frisch and Screaton, 2001; Green and Kroemer, 2004]. These stimuli trigger different intracellular signals leading to apoptosis, that often involve the activation of caspases through two main pathways. Both death receptor and mitochondrial pathways converge at the level of effector-caspase activation. Then, the apoptotic programme branches into a multitude of sub-programmes, the sum of which results in the ordered dismantling of the cell. However, although caspases are important in mediating apoptosis, recent studies indicate caspases not to be required for all forms of cell-death and their activation not always leading to cell-death [Abraham and Shaham, 2004]. Such data have clinical implications. For example, the efficacy

of caspase inhibitor treatment on acute organ dysfunction following ischemic/reperfusion injury is dependent upon a major role of caspases in apoptosis [Iwata et al., 2002]. In cancer, the elucidation of apoptosis in the absence of caspase activity may identify new pharmacological targets for cancer treatment [Johnstone et al., 1999; Kolenko et al., 2000]. With regard to this, it has been reported that STS-induced apoptosis in several cancer cell lines does not require caspase activity [Nutt et al., 2002; Cummings et al., 2004]. We showed here that induction of apoptotic changes by STS requires caspase activity in both nontumorigenic (HaCaT) and neoplastic (HT-29) epithelial cell lines. In general, the effect of STS was more rapid in keratinocytes as well as the consequences of caspase inhibition were more pronounced. However, both induction of apoptosis and cleavage of Dsg2 were clearly related to caspase activity also in tumorigenic HT-29.

In epithelia, cadherin complexes are the main mediators of intercellular adhesion [Green and Gaudry, 2000; Ishii and Green, 2001].

The extracellular domains of desmosomal cadherins interact in a calcium-dependent manner, whereas the cytoplasmic domain serves as a membrane anchor for Pg, Pkp, and Dpk, that ultimately connect the desmosomal plaque with the keratin cytoskeleton. As the cells undergo apoptosis, desmosome is dismantled by the targeted proteolysis of its constituents. In most cases, the cleavage of desmosomal proteins is orchestrated by caspases, leading to dissolution of cell structure and morphology [Weiske et al., 2001]. In this study we demonstrated that, upon induction of apoptosis by STS, caspase 3 mediates the intracellular cleavage of Dsg2 leading to its progressive depletion from the cell and accumulation of a 70-kDa fragment into the cytosol. These results were obtained through targeted pharmacological approaches in both HaCaT keratinocytes and HT-29 enterocytes, thus demonstrating that the apoptotic proteolysis of Dsg2 occurs in a similar fashion in both stratified and simple epithelia, respectively. Furthermore, the pivotal role of Dsg2 in cell-cell adhesion among keratinocytes is corroborated by the correlation between Dsg2 cleavage and loss of intercellular adhesion, although further studies are needed to shed more light on this field.

In conclusion, in this study, we showed for the first time that Dsg2 is targeted for proteolysis during STS-induced, caspase-mediated apoptosis. The fate of Dsg2 depends on caspase 3 activity and its proteolysis correlates well with the reduction of intercellular adhesion strength in keratinocyte and enterocyte cell lines.

## REFERENCES

- Abraham MC, Shaham S. 2004. Death without caspases, caspases without death. *Trends Cell Biol* 14:184–193.
- Arredondo J, Chernyavsky AI, Karaoui A, Grando SA. 2005. Novel mechanisms of target cell death and survival and of therapeutic action of IVIG in pemphigus. *Am J Pathol* 167:1531–1544.
- Awad MM, Dalal D, Cho E, Amat-Alarcon N, James C, Tichnell C, Tucker A, Russell SD, Bluemke DA, Dietz HC, Calkins H, Judge DP. 2006. DSG2 mutations contribute to arrhythmogenic right ventricular dysplasia/cardiomyopathy. *Am J Hum Genet* 79:136–142.
- Beutler B. 2001. Autoimmunity and apoptosis: The Crohn's connection. *Immunity* 15:5–14.
- Biedermann K, Vogelsang H, Becker I, Plaschke S, Siewert JR, Hofer H, Keller G. 2005. Desmoglein 2 is expressed abnormally rather than mutated in familial and sporadic gastric cancer. *J Pathol* 207:199–206.
- Brancolini C, Sgorbissa A, Schneider C. 1998. Proteolytic processing of the adherens junctions components beta-catenin and gamma-catenin/plakoglobin during apoptosis. *Cell Death Differ* 5:1042–1050.
- Chitaev NA, Troyanovsky SM. 1997. Direct Ca<sup>2+</sup>-dependent heterophilic interaction between desmosomal cadherins, desmoglein and desmocollin, contributes to cell-cell adhesion. *J Cell Biol* 138:193–201.
- Cirillo N, Femiano F, Gombos F, Lanza A. 2006. Serum from pemphigus vulgaris reduces desmoglein 3 half-life and perturbs its de novo assembly to desmosomal sites in cultured keratinocytes. *FEBS Lett* 580:3276–3281.
- Cirillo N, Gombos F, Lanza A. 2007. Changes in desmoglein 1 expression and subcellular localization in cultured keratinocytes subjected to anti-desmoglein 1 pemphigus autoimmunity. *J Cell Physiol* 210:411–416.
- Cummings BS, Kinsey GR, Bolchoz LJC, Schnellmann RG. 2004. Identification of caspase-independent apoptosis in epithelial and cancer cells. *J Pharmacol Exp Ther* 310:126–134.
- Dusek RL, Getsios S, Chen F, Park JK, Amargo EV, Cryns VL, Green KJ. 2006. The differentiation-dependent desmosomal cadherin desmoglein 1 is a novel caspase-3 target that regulates apoptosis in keratinocytes. *J Biol Chem* 281:3614–3624.
- Eshkind L, Tian Q, Schmidt A, Franke WW, Windoffer R, Leube RE. 2002. Loss of desmoglein 2 suggests essential functions for early embryonic development and proliferation of embryonal stem cells. *Eur J Cell Biol* 81:592–598.
- Frisch SM, Screaton RA. 2001. Anoikis mechanisms. *Curr Opin Cell Biol* 13:555–562.
- Garrod DR, Merritt AJ, Nie Z. 2002. Desmosomal cadherins. *Curr Opin Cell Biol* 14:537–545.
- Green KJ, Gaudry CA. 2000. Are desmosomes more than tethers for intermediate filaments? *Nat Rev Mol Cell Biol* 1:208–216.
- Green DR, Kroemer G. 2004. The pathophysiology of mitochondrial cell death. *Science* 305:626–629.
- Hengartner MO. 2000. The biochemistry of apoptosis. *Nature* 407:770–776.
- Ishii K, Green KJ. 2001. Cadherin function: Breaking the barrier. *Curr Biol* 11:R569–R572.
- Iwata A, Harlan JM, Vedder NB, Winn RK. 2002. The caspase inhibitor z-VAD is more effective than CD18 adhesion blockade in reducing muscle ischemiareperfusion injury: Implication for clinical trials. *Blood* 100:2077–2080.
- Johnstone RW, Cretney E, Smyth MJ. 1999. P-glycoprotein protects leukemia cells against caspase-dependent, but not caspase-independent, cell death. *Blood* 93:1075–1085.
- Kaplan MJ. 2004. Apoptosis in systemic lupus erythematosus. *Clin Immunol* 112:210–218.
- Kerr JF, Wyllie AH, Currie AR. 1972. Apoptosis: A basic biological phenomenon with wide-ranging implications in tissue kinetics. *Br J Cancer* 26:239–257.
- King IA, Angst BD, Hunt DM, Kruger M, Arnemann J, Buxton RS. 1997. Hierarchical expression of desmosomal cadherins during stratified epithelial morphogenesis in the mouse. *Differentiation* 62:83–96.
- Kljuic A, Bazzi H, Sundberg JP, Martinez-Mir A, O'Shaughnessy R, Mahoney MG, Levy M, Montagutelli X, Ahmad W, Aita VM, Gordon D, Uitto J, Whiting D, Ott J, Fischer S, Gilliam TC, Jahoda CA, Morris RJ,



- Panteleyev AA, Nguyen VT, Christiano AM. 2003. Desmoglein 4 in hair follicle differentiation and epidermal adhesion: Evidence from inherited hypotrichosis and acquired pemphigus vulgaris. *Cell* 113:249–260.
- Kolenko VM, Uzzo RG, Bukowski R, Finke JH. 2000. Caspase-dependent and -independent death pathways in cancer therapy. *Apoptosis* 5:17–20.
- Kurzen H, Munzing I, Hartschuh W. 2003. Expression of desmosomal proteins in squamous cell carcinomas of the skin. *J Cutan Pathol* 30:621–630.
- Lanza A, Cirillo N. 2007. Caspase-dependent cleavage of desmoglein 1 depends on the apoptotic stimulus. *Br J Dermatol* 156:400–402.
- Lanza A, Femiano F, De Rosa A, Cammarota M, Lanza M, Cirillo N. 2006. The N-terminal fraction of desmoglein 3 encompassing its immunodominant domain is present in human serum: Implications for pemphigus vulgaris autoimmunity. *Int J Immunopathol Pharmacol* 19:399–407.
- Lockshin RA, Williams CM. 1965. Programmed cell death—I. Cytology of degeneration in the intersegmental muscles of the Pernyi Silkmoth. *J Insect Physiol* 11: 123–133.
- Nutt LK, Chandra J, Pataer A, Fang B, Roth J, Swisher SG, O'Neil RG, McConkey DJ. 2002. Bax-mediated  $Ca^{2+}$  mobilization promotes cytochrome c release during apoptosis. *J Biol Chem* 277:20301–20308.
- Saraste A, Pulkki K. 2000. Morphologic and biochemical hallmarks of apoptosis. *Cardiovasc Res* 45:528–537.
- Schafer S, Stumpp S, Franke WW. 1996. Immunological identification and characterization of the desmosomal cadherin Dsg2 in coupled and uncoupled epithelial cells and in human tissues. *Differentiation* 60:99–108.
- Schwarz MA, Owaribe K, Kartenbeck J, Franke WW. 1990. Desmosomes and hemidesmosomes: Constitutive molecular components. *Annu Rev Cell Biol* 6:461–491.
- Strasser A, Harris AW, Bath ML, Cory S. 1990. Novel primitive lymphoid tumours induced in transgenic mice by cooperation between myc and bcl-2. *Nature* 348:331–333.
- Thornberry NA, Lazebnik Y. 1998. Caspases: Enemies within. *Science* 281:1312–1316.
- Weiske J, Schöneberg T, Schröder W, Hatzfeld M, Tauber R, Huber O. 2001. The fate of desmosomal proteins in apoptotic cells. *J Biol Chem* 276:41175–41181.